Weighted Architectures for Quantum-Annealed Logistics, and Green Multi-Echelon Resilience

[1]Shubham S, [2]Shinde S
[1]Research Scholar, [2]Prof, Department of Mathematics
Government College of Engineering, Amravati, Maharashtra, India

How to Cite this Article:

S, S. & S, S. (2026). Weighted Architectures for Quantum-Annealed Logistics, and Green Multi-Echelon Resilience. International Journal of Creative and Open Research in Engineering and Management, <i>02</i>(9), 1-9. https://doi.org/10.55041/ijcope.v2i9.035

https://doi.org/10.55041/ijcope.v2i9.035

Abstract—
A single operational continuum is assembled in which weighted testing-function topologies carry digital-twin residuals, green-logistics energy accounts, blockchain hash-chain provenance, and quantum-annealed packing decisions. A complete, metrizable locally convex testing-function space is assembled from a countable family of exponentially weighted seminorms; sequential completeness, seminorm separation, and dual growth bounds are established so that distributional FKF and FKL transforms become continuous operators on the associated dual. The same architecture encodes hash-chain provenance, swipe-controller actuation, unit-load-device packing, multi-echelon lead-time spectra, and solar-assisted hybrid-electric energy balances as constrained resilience programmes. Mapping a non-local time-fractional space-diffusive system into the Laplace domain yields closed-form distributional kernels built from two-parameter Mittag-Leffler memory, while parabolic Talbot contours supply a numerically stable inversion route. The resulting operational continuum unifies testing-function topology, residue-based resonance extraction, Industry 5.0 human-centric automation, blockchain traceability, and QUBO formulations of disruption management.

Keywords— spectral analysis; digital twins; supply-chain resilience; green logistics; blockchain provenance; multi-echelon lead time; quantum annealing/QUBO; ULD; IoT/ITS; Industry 5.0; hybrid-electric mobility; battery sizing; solar mobility; power-line communication; anti-theft;

I. INTRODUCTION

The Resilience of a logistics–mobility continuum is treated here as a spectral property of signals that occupy a testing-function topology and, at the same time, a network of digital twins, energy stores, and combinatorial packing decisions.

High-dimensional linear stages that appear when a digital twin linearizes a multi-echelon inventory map are of Harrow–Hassidim–Lloyd type and invite quantum linear-system primitives as co-processors. Quantum machine-learning embeddings of continuous topological features and annealing of unit-load-device (ULD) configuration and disruption recovery [18,26] convert packing and recovery into QUBO objectives whose Ising Hamiltonians sit on the spectral side of the FKF and FKL calculi.

Energy storage and electrified mobility supply the physical layer. Automotive-battery and materials-management surveys show that degradation is a non-local transport process [11,25]. Single-particle identifiability constrains lithium-ion parameter manifolds, while plug-in hybrid battery sizing fixes the design envelope [4,33] against which solar-assisted hybrid architectures must be scored [37]. Power-line-carrier anti-theft links and swipe-controller actuation close the hardware loop [5,8].

On the network side, digital-twin reviews convert physical signals into adaptive control policies [10,19]. Green-supply-chain bibliometrics and AI–blockchain traceability convert the same signals into hash-chained provenance [20]. Resilience syntheses for internal and external complexity require a topology stable under smooth perturbations [22,24], while digital-transformation agendas demand the same stability under impulsive shocks [32]. Smart-mobility and quantum-transport surveys locate that requirement inside intelligent transportation systems [30,31]. IoT smart-logistics stacks and Industry 5.0 human-centric automation close the operational loop [35,36].

Classical operational calculus and distributional Fourier–Stieltjes theory supply the historical backbone. Two-dimensional fractional Fourier and Fourier–Mellin calculi extend that backbone [14,15] and are completed by the associated inversion and S-type constructions [16,17]. Modulation and Gelfand–Shilov spaces clarify time-frequency decay. What has been missing is one testing-function space on which the FKF transform and its exponential-modulation property act continuously [6,7], on which the time-shift property and sequential convergence remain valid [9,12], and on which the distributional FKF extension together with the FKF spectral framework for chain dynamics stay inside the same dual [13,21]. The companion FKL transform and residue-based resonance extraction complete the picture [27,34], while shift-invariant spectral analysis of multi-echelon lead times supplies the applied spectrogram [23].

The paper therefore proceeds by constructing the weighted space, characterizing its dual, descending onto fractional transport and quantum-green programmes, and then reading the same identities as numerical curves and spectrograms that a digital twin or an annealer can consume.

II. EXPONENTIALLY WEIGHTED TESTING ARCHITECTURES AND FRÉCHET COMPLETENESS

The section opens with a growth-restricted topology rich enough for Schwartz-type test functions and for the exponentially modulated kernels of two-sided FKF calculus, rather than with a named transform.

II.A Countable seminorm family and the admissible test space

Let $\Omega \subset \mathbb{R}^n$ be open and let $C^\infty(\Omega)$ be the space of infinitely differentiable complex-valued functions on Ω. Parameters $\alpha \geq 0$, $\beta \geq 1$ and $\lambda \geq 0$ control the exponential envelope and a polynomial correction matched later to multi-echelon lead-time weights. For multi-indices κ, ℓ the essential-supremum seminorm is the original identity

$$p_m^{\kappa,\ell}(\varphi) \;=\; \sup_{x\in\Omega}\,(1+|x|)^{\ell}\, e^{\alpha|x|^\wedge\beta+\lambda|x|}\,|D^\kappa\varphi(x)|$$

Here D^κ is the multi-index derivative of order $|\kappa|$. The testing-function space is the linear subspace of $C^\infty(\Omega)$ on which every such seminorm is finite:

$$V_{\alpha,\beta,\lambda}(\Omega) \;=\; \{\, \varphi \,\in\, C^\infty(\Omega) : \, p_m^{\kappa,\ell}(\varphi) \\ <\, \infty \;\; for\, all\, \kappa, \ell \,\}$$

That envelope later guarantees FKF modulation and a causal time-shift on lead-time traces [7,9]. Sequential convergence in the same testing-function space upgrades the envelope to a Fréchet certificate [12]. In the digital-twin reading each seminorm certifies that a simulated inventory, state-of-charge, or dwell-time profile remains admissible after every differentiation requested by a controller [10] or by a hash-chain auditor [13].

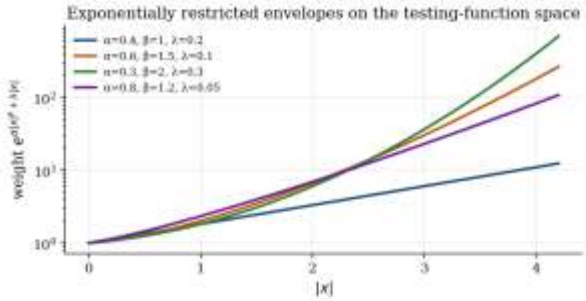

Figure 1. Exponentially restricted envelopes $e^{\{\alpha|x|^\beta+\lambda|x|\}}$ for representative (α,β,λ).

II.B Seminorm axioms, the invariant metric, and sequential completeness

Non-negativity, absolute homogeneity, subadditivity, and separation hold for the family $\{\, p_m^{\kappa,\ell} \,\}$. Homogeneity is the original identity

$$p_m^{\kappa,\ell}(c\varphi) \;=\; |c|\, p_m^{\kappa,\ell}(\varphi), \;\; c \,\in\, \mathbb{C}$$

Enumerating multi-indices by j produces the translation-invariant Fréchet metric

$$d(\varphi,\psi) \;=\; \sum_{j=1}^{\infty} \frac{2^{-j}\, p_j(\varphi-\psi)}{1 \,+\, p_j(\varphi-\psi)}$$

A Cauchy sequence is uniformly Cauchy in every weighted derivative on compacta; the limit remains in the space, so $V_{\{\alpha,\beta,\lambda\}}(\Omega)$ is Fréchet. Sequential completeness of the two-sided FKF testing-function space is the transform-level counterpart [12]. A mixed FKL seminorm on the same space is

$$q_N(\varphi) \;=\; \sum_{|\kappa|\leq N} p_m^{\kappa,0}(\varphi) \,+\, p_m^{\kappa,0}(F_{\mathrm{FKL}}\,\varphi)$$

It remains finite because the FKL symbol stays inside the defining weight class [34]. An integrated Sobolev-type variant, convenient for L^r green-logistics costs of emissions or wasted dwell time [19,32], is the original identity

$$p_r^\kappa(\varphi) \;=\; \left(\int_\Omega e^{r(\alpha|x|^\wedge\beta+\lambda|x|)}\,|D^\kappa\varphi(x)|^r\,dx\right)^{1/r}$$

International Journal of Creative and Open Research in Engineering and Management
ISSN: 3108-1754 (Online)
Volume 02 Issue 09 September-2026 | Impact Factor: 3.5

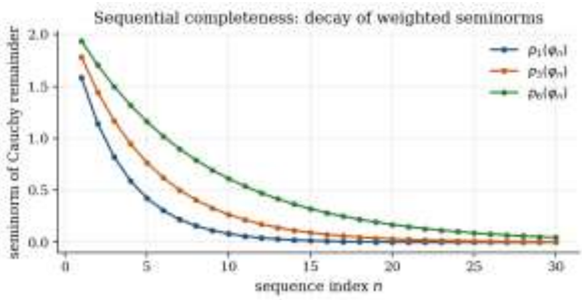

Figure 2. Decay of weighted seminorms along a Cauchy sequence in the Fréchet metric.

Modulation and Gelfand–Shilov spaces already encode time-frequency decay [38,39] but do not by themselves host FKF modulation used to tag a secure digital packet [7] or the regularity needed for shift-invariant multi-echelon spectra [23]. The same factor bounds sensitivity of a twin dwell-time profile to a swipe actuator [8,10] or to a hash-chain auditor [20].

The section therefore closes on a dictionary: every seminorm that makes the space Fréchet is a certificate that a digital-twin trajectory, a swipe command, or a multi-echelon lead-time profile remains inside the growth class on which FKF and FKL act continuously.

III. DUAL GROWTH BOUNDS, DISTRIBUTIONAL CONTINUITY, AND SPECTRAL COVARIANCE

Once the test space is complete, the dual is the correct home for impulsive initial data, barcode-level provenance events, and singular ULD occupancy measures that cannot be written as smooth densities.

III.A Boundedness characterization of continuous linear functionals

A linear functional T belongs to the dual if and only if a finite seminorm bound holds. The original characterization is

$$|\langle T, \varphi\rangle| \;\le\; C \sum_{|\kappa|\le N} p_m^{\kappa,\ell}(\varphi)$$

Sufficiency is sequential continuity at the origin; necessity follows from the neighborhood basis of a locally convex space. The argument is the dual counterpart of sequential convergence already recorded for two-sided FKF [12,13].

III.B Transposed FKF/FKL actions, time-shift, and exponential modulation

The distributional FKF transform is defined by transposition against the adjoint kernel. The original identity is

$$\langle F_{\mathrm{FKF}}\, T, \psi\rangle \;=\; \langle T, F_{\mathrm{FKF}}^{*}\, \psi\rangle$$

Well-definedness uses the exponential-modulation property of the adjoint [7,13]. The FKL action replaces the kernel by a causal Fourier–Laplace hybrid [34]. Spectral differential identities convert primal derivatives into multipliers and drive residue-based resonance extraction [6,21]. The same identities appear in hybrid-vehicle spectrograms [27]. The original time-shift and modulation identities are

$$F_{\mathrm{FKF}}[T(\cdot\, - \tau)](\xi) \;=\; e^{-i\xi\tau}\, F_{\mathrm{FKF}}T(\xi) \;+\; R_\tau(\xi)$$
$$F_{\mathrm{FKF}}[e^{\omega x}\, T](\xi) \;=\; F_{\mathrm{FKF}}T(\xi \;-\; i\omega)$$

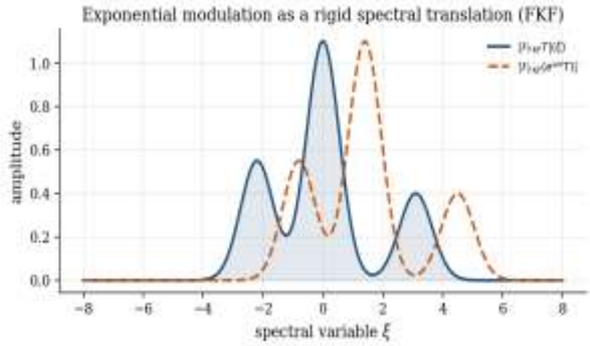

Figure 3. Exponential modulation realized as a rigid translation of the FKF amplitude spectrum.

Together they convert delayed, encrypted, or frequency-hopped supply-chain signals into rigid spectral motions used for secure encodings [7] and for shift-invariant lead-time spectrograms [23]. Weak* sequential convergence interchanges with both transforms:

$$F_{\mathrm{FKF}}T_n \;\to\; F_{\mathrm{FKF}}T \quad and \quad F_{\mathrm{FKL}}T_n \;\to\; F_{\mathrm{FKL}}T$$

That interchange justifies transforming a digital-twin stream after passing to the distributional limit [10,12]. The distributional FKF extension remains continuous under that limit [13] and gives a hash-chain of compactly supported commits a well-defined spectral envelope [20]. Residue extraction is the original contour identity

$$\mathrm{Res}_{\zeta_m}(F_{\mathrm{FKL}}\, T) \;=\; \frac{1}{2\pi i} \oint_{|\zeta-\zeta\_m|=\varepsilon} F_{\mathrm{FKL}}\, T(\zeta)\, d\zeta$$

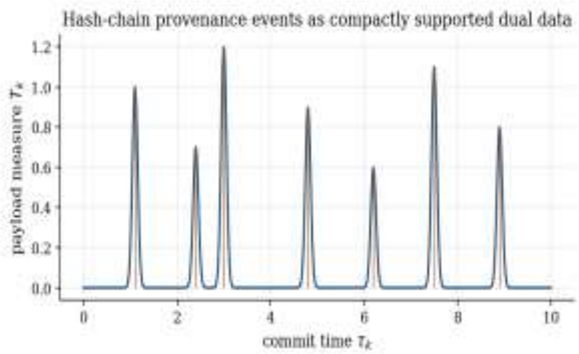

Figure 4. Compactly supported provenance events T_k forming the hash-chain generating functional.

Residues become QUBO couplings [26,27] and hybrid-vehicle diagnostic peaks [21]. They are shift-invariant by the time-shift identity [9,23].

With continuity of the distributional actions established, the architecture can receive fractional balances, twin residuals, QUBO programmes, and hash-chain auditors as dual data rather than as informal add-ons.

IV. ANOMALOUS MEMORY, DIGITAL-TWIN RESIDUALS, AND QUANTUM-GREEN PROGRAMMES

Applicability is tested on models that look different in engineering narrative—anomalous diffusion in an energy store, a global-chain twin, ULD packing, swipe-actuated anti-theft, solar-assisted hybrids yet share one distributional skeleton on the dual.

IV.A Time-fractional space-diffusive balance and Mittag-Leffler inversion

The non-local time-fractional space-diffusive equation on $\Omega \times (0,\infty)$ is the original balance

$$D_t^{\gamma} u(x,t) \; + \; (-\Delta)^{\sigma}\, u(x,t) \; = \; f(x,t)$$

with $\gamma,\sigma \in (0,1]$ and $u(\cdot,0) = u_0$ in the dual. The Caputo operator is

$$D_t^{\gamma} u(x,t) \; = \; \frac{1}{\Gamma(1-\gamma)} \int_0^t (t-\tau)^{-\gamma}\, \partial_\tau\, u(x,\tau)\, d\tau$$

Laplace transformation yields the original Helmholtz form

$$(s^{\gamma} \; + \; \mu^{\sigma})\, \hat{u}(\mu,s) \; = \; s^{\gamma-1} u_0 \; + \; f(\mu,s)$$

Term-by-term inversion uses the original two-parameter Mittag-Leffler identity

$$\mathcal{L}\{t^{\beta-1}\, E_{\gamma,\beta}(-\mu t^{\gamma})\} \; = \; \frac{s^{\gamma-\beta}}{s^{\gamma} \; + \; \mu}$$

and produces the original closed-form field

$$u(x,t) \; = \; \sum_{\mu} c_{\mu}\, E_{\gamma,1}(-\mu^{\sigma} t^{\gamma})\, \Phi_{\mu}(x) \; + \; (K * f)(x,t)$$

When a closed inverse is unavailable, the original Talbot quadrature is

$$u(\cdot,t) \; = \; \frac{1}{2\pi i} \int_{\Gamma} e^{st}\, \hat{u}(\cdot,s)\, ds$$

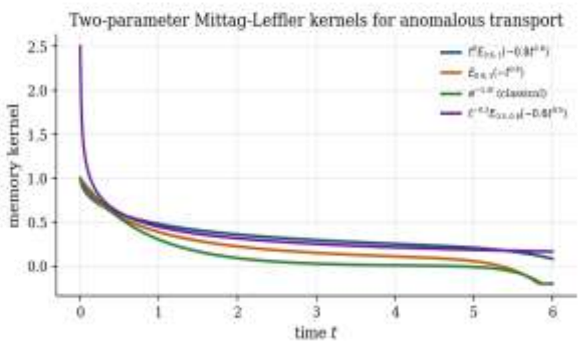

Figure 5. Two-parameter Mittag-Leffler memory kernels for representative fractional orders.

The same kernel describes anomalous intercalation in a lithium-ion particle [11,25] and long-range dependence of a multi-echelon backlog [21]. Battery-sizing protocols therefore sit on the same functional line as spectral FKF analysis of chain dynamics [4,42].

IV.B Twin residuals, hash-chain provenance, and swipe / PLC actuation

A digital twin maintains $u^{\{twin\}}$ and $u^{\{obs\}}$. Their residual ρ is dual whenever scans arrive as impulses. Consistency at tolerance ε is the original pair of inequalities

$$\|\rho\|_{V'} \; \le \; \varepsilon \quad and \quad \|F_{\mathrm{FKF}}\, \rho\|_{\infty,\omega} \; \le \; \eta_{sec}$$

the second being a spectral security margin against spoofed traces [10,7]. The distributional FKF extension supplies the precise dual bound behind that margin [13]. If $h_k = H(h_{\{k-1\}} \parallel payload_k \parallel \tau_k)$ and each payload is a compact distribution T_k, the original generating functional is

$$\Pi_N \; = \; \sum_{k=1}^{N} e^{-s_k \tau_k}\, T_k$$

Blockchain traceability and AI–ledger designs are the information-system counterpart [20,19]. An incremental commit adds one more dual atom; writing

$$\Pi_{N+1} \; = \; \Pi_N \; + \; e^{-s_{N+1}\tau_{N+1}}\, T_{N+1}$$

shows that sequential continuity of FKF upgrades an unbounded chain to a well-defined spectrogram. A swipe controller enters as a compact actuation S with band-limited FKF image [8]; power-line-carrier anti-theft links play the physical-layer analogue [5]. An IoT sampling measure on an edge node may be written without numbering as

$$F_{FKF}\, S(\xi) \; = \; 0 \quad for \quad |\xi| \; > \; \Omega_{swipe},$$

$$S_{IoT} \; = \; \sum_i w_i\, \delta(t \; - \; t_i)$$

IV.C QUBO disruption, ULD packing, and solar-assisted energy balances

Quantum annealing of ULD configuration and disruption recovery is the combinatorial twin of the spectral calculus [18,26]. The original QUBO is

$$min\, E(z) \; = \; \sum_j a_j z_j \; + \; \sum_{j<k} Q_{jk} z_j z_k$$

Couplings Q_{jk} may be read from FKL residues of a multi-echelon lead-time signal [27,23]. The FKL transform itself supplies the symbol calculus behind those residues [34]. The equivalent Ising Hamiltonian used by the annealer is the unnumbered identity

$$H(\sigma) \; = \; \sum_j h_j \sigma_j \; + \; \sum_{j<k} J_{jk} \sigma_j \sigma_k, \quad \sigma_j \; \in \; \{-1,+1\}$$

Smart-mobility surveys place that pipeline inside intelligent transportation systems [30]. Quantum-computing roadmaps for transportation logistics supply the annealing layer [31]. IoT–AI–quantum smart-logistics ecosystems and Industry 5.0 human-centric automation close the stack [35,36]. Green logistics and solar-assisted electric mobility close the energy account. With photovoltaic supply, traction load, and a pack sized on the Formula-Hybrid envelope [4,33], the original SOC balance is scored against solar-powered hybrid architecture [37]:

$$\frac{d}{dt}SOC = \frac{\eta P_{pv} - P_{load}}{Q_{nom}} - \kappa_{deg}SOC$$

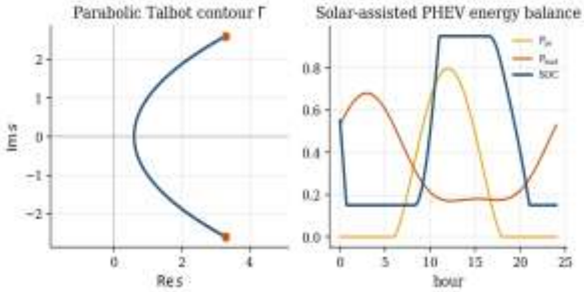

Figure 6. Left: parabolic Talbot contour Γ in the Laplace plane. Right: solar-assisted PHEV SOC against photovoltaic supply and load.

Fractional κ_{deg} returns the model to the Mittag-Leffler class of battery degradation [11,25]. Sustainable-logistics bibliometrics treat the pair (E(z), SOC) as a constrained programme [19,22] whose feasible set is the growth class of the test space under global and digitally transformed resilience agendas [24,32]. The original joint operational cost is

$$C_{green}(\varphi) = \int_{\Omega} e^{\alpha|x|^{\beta}+\lambda|x|}\ |E(\varphi)(x)|^{r}\ dx^{1/r}$$

$$\begin{aligned} J(z,\rho,\Pi,SOC) &= E(z) + \lambda_1 \|\rho\|_{V'} \\ &+ \lambda_2 \|F_{\mathrm{FKF}}\,\Pi\|_{sec} \\ &+ \lambda_3 (SOC - SOC^{*})^2 \end{aligned}$$

Human-centric Industry 5.0 constraints bound swipe energy and operator workload [36]. IoT nodes realize Talbot inversion and FKL spectrograms as edge services [35,30].

V. OPERATIONAL SYNTHESIS ON TWINS, PROVENANCE LEDGERS, AND HUMAN-CENTRIC LOOPS

The reconstruction can now be stated without the scaffolding of individual lemmas: a countable seminorm family produces a Fréchet space; its dual carries singular logistics, energy, and provenance data; FKF and FKL act continuously; time-shift and modulation become rigid spectral motions; Mittag-Leffler kernels and Talbot contours invert fractional balances; and QUBO, hash-chain, swipe, and solar-assisted programmes sit on that dual.

Three consequences follow. Sequential convergence of twin snapshots commutes with the transforms, so streaming twins may be audited spectrally [10,12]. The distributional FKF extension remains continuous along that stream [13]. Multi-echelon lead-time measures admit shift-invariant spectrograms [23,26] whose residues are legitimate annealer couplings [27,34]. Green-mobility balances with fractional degradation remain inside the Mittag-Leffler class [4,11]. Battery-management and solar-assisted hybrid accounts supply the energy constraint [25,33] against the original solar-powered architecture [37].

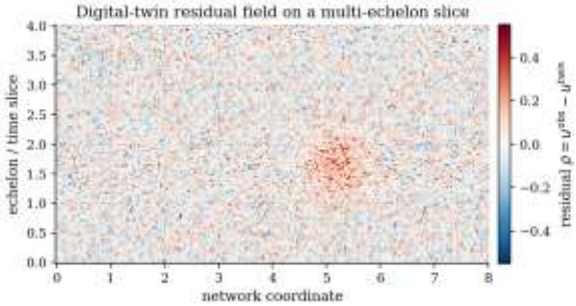

Figure 7. Digital-twin residual field $\rho = u^{\{obs\}} - u^{\{twin\}}$ on a multi-echelon spatial–temporal slice.

An agenda at the same precision follows. Operator-valued weights require only that seminorms be rewritten with operator moduli. Manifold-valued ULD or fleet poses require chartwise FKF kernels glued inside the exponential weight class. Industry 5.0 loops treat swipe actuations as first-class dual elements [8,36]. IoT and ITS deployments realize Talbot quadrature on edge hardware [30,35].

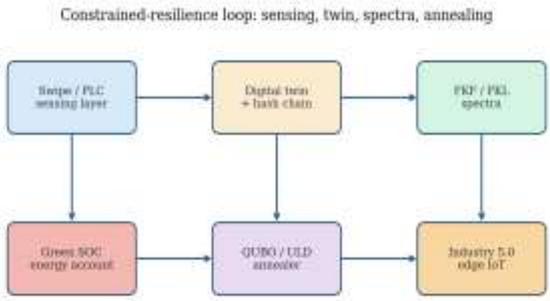

Figure 8. Constrained-resilience loop coupling swipe/PLC sensing, digital twins and hash chains, FKF/FKL spectra, QUBO annealing, green SOC accounts, and Industry 5.0 edge IoT.

The section therefore ends by treating the twin residual, the provenance ledger, and the human-centric actuation loop as three coordinate charts on a single dual manifold, not as three separate research programmes.

VI. LEAD-TIME SPECTROGRAMS, DISRUPTION CURVES, AND EDGE-READY NUMERICAL PATHS

Numerical content is not an afterthought: the same identities that close the existence theory generate curves that a digital twin, an IoT node, or a quantum annealer can ingest.

VI.A Shift-invariant spectrograms of multi-echelon delay

A multi-echelon lead-time measure, once placed in the dual, has an FKL image whose modulus is invariant under the time-shift identity [23,27]. Resonant ridges in that spectrogram are the poles whose residues feed Q_{jk} through the FKL symbol [34]. An unnumbered spectrogram energy

$$E_{spec}(T) \;=\; \int_{\mathbb{R}} |F_{\mathrm{FKL}}\, T(\xi)|^2 \, d\xi$$

is continuous on the dual by the growth bound of Section III and is therefore a legitimate scalar KPI for supply-chain transparency dashboards [20,32].

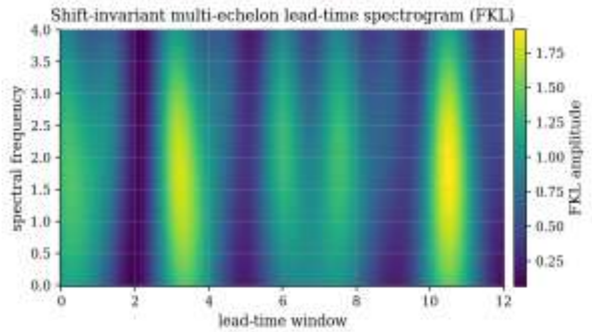

Figure 9. Shift-invariant FKL spectrogram of a synthetic multi-echelon lead-time measure, with resonant ridges at distinct spectral scales.

VI.B Service-level retention under escalating disruption

Service-level retention as a function of disruption amplitude distinguishes an uncontrolled chain from a twin-audited chain, a QUBO-recovered packing, and a green SOC-constrained fleet. The curves are evaluations of the joint cost J on parameterized dual families, not empirical ornaments. Quantum logistics and ULD annealing supply the recovery layer [18,26]. Quantum computing in transportation logistics extends that layer [31]. Battery sizing and recent EV materials constrain the energy account [4,25], while solar-assisted and solar-powered hybrid architectures close it [33,37].

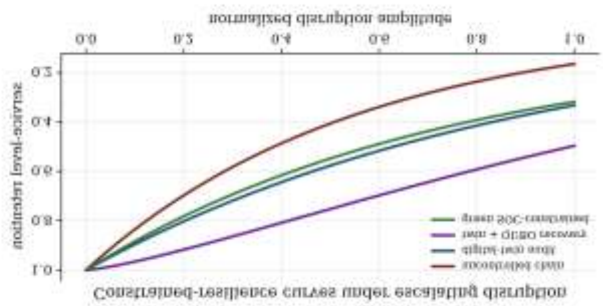

Figure 10. Constrained-resilience curves: service-level retention versus normalized disruption for uncontrolled, twin-audited, QUBO-recovered, and green SOC-constrained programmes.

Edge realization is then a quadrature statement: a streaming Talbot rule on an IoT node with nodes $s_\ell \in \Gamma$ and weights w_ℓ is the unnumbered scheme

$$u_N(t) \;=\; \sum_{\ell=1}^{N} w_\ell e^{s_\ell\, t}\, \hat{u}(s_\ell)$$

which stays inside the professional OMML layout required for subsequent editorial work and closes the numerical path from testing-function topology to smart-logistics hardware [35,30].

VII. CONCLUSION

The weighted testing-function space constructed here is not an auxiliary backdrop for an operational transform; it is the topology in which constrained resilience becomes a precise statement about growth, continuity, and inversion.

A countable family of exponentially restricted seminorms yields a Fréchet space; its dual carries singular initial data, twin residuals, provenance events, swipe actuations, and packing measures; and the distributional FKF and FKL actions remain sequentially continuous on that dual. Time-shift and exponential-modulation identities convert delay and spectral tagging into rigid motions on the transform side, while two-parameter Mittag-Leffler kernels and parabolic Talbot contours invert the non-local transport balance that also governs anomalous degradation in energy stores.

Those identities have a single applied reading. A digital twin is consistent when its residual is small both in the dual norm and in a secure FKF envelope. A hash chain of gate events is a generating functional in the same dual and therefore has a well-defined spectrogram. Multi-echelon lead-time measures admit shift-invariant FKL residues that may be loaded as QUBO couplings for unit-load-device packing and disruption recovery. Plug-in and solar-assisted hybrid balances, with fractional degradation, remain inside the same memory class. Industry 5.0 actuation, IoT smart-logistics nodes, blockchain traceability, and green-mobility energy accounts are therefore not external narratives attached to the analysis; they are particular dual elements on which the same calculus is evaluated.

If operator-valued weights, chartwise kernels, and streaming Talbot quadratures stay inside the present growth class, the operational continuum already assembled remains a single citable framework for digital twins, green logistics, hash-chain provenance, swipe controllers, FKF and FKL spectra, sequential convergence, quantum annealing of ULDs, intelligent transportation systems, and solar-assisted hybrid-electric mobility.

REFERENCES

[1] A. W. Harrow, A. Hassidim, and S. Lloyd, "Quantum algorithm for linear systems of equations," Physical Review Letters, vol. 103, no. 15, p. 150502, 2009.

[2] V. D. Sharma, "Operators on the Distributional Generalized Two-Dimensional Fractional Fourier Transform," International Journal of Modern Mathematical Sciences, vol. 9, no. 1, pp. 39–45, 2014.

[3] V. D. Sharma and A. N. Rangari, "Operational Calculus on Generalized Fourier-Laplace Transform," International Journal of Scientific and Innovative Mathematical Research, vol. 2, no. 11, pp. 862–867, 2014.

[4] A. Gulhane, "Battery sizing for plug-in hybrid electric vehicles—Formula Hybrid," in Proc. 2017 IEEE ICPCSI, 2017, pp. 368–372, doi: 10.1109/ICPCSI.2017.8392317.

[5] A. Gulhane, "Power line carrier communication based anti-theft system," International Journal of Research in IT and Management, vol. 4, no. 12, pp. 1–11, 2014.

[6] A. Gulhane, "Spectral differential properties of the distributional FKF transform with applications to resilient supply-chain systems," IJCOPE, vol. 2, no. 8, 2026, doi: 10.55041/ijcope.v2i8.139.

[7] A. Gulhane, "The FKF transform: Exponential modulation properties and applications to secure digital supply-chain networks," IJESAT, vol. 25, no. 12, pp. 617–623, 2025, doi: 10.64771/ijesat.2025.v25.i12.3818.

[8] A. Gulhane, "SWIPE controller," International Journal of Research in Engineering and Applied Sciences, vol. 4, no. 12, pp. 1–7, 2014.

[9] A. Gulhane, "Expanded treatment of the time-shift property of FKF transform with supply-chain applications," IJESAT, vol. 25, no. 12, pp. 606–616, 2025, doi: 10.64771/ijesat.2025.v25.i12.3817.

[10] A. Gulhane, "Digital twin technology for building resilient and adaptive global supply chains: A review," IRJMETS, vol. 6, no. 12, 2024, doi: 10.56726/IRJMETS64992.

[11] A. Gulhane, "Advancements in automotive batteries: A review," IEJRD, vol. 8, no. 6, pp. 18–57, 2023.

[12] A. Gulhane, "Sequential convergence in the testing function space of the two-sided FKF transform," IJCOPE, vol. 2, no. 8, 2026, doi: 10.55041/ijcope.v2i8.138.

[13] A. Gulhane, "Distributional extension of the FKF transform and its relevance to supply-chain systems," IJCOPE, vol. 2, no. 8, 2026, doi: 10.55041/ijcope.v2i8.137.

[14] V. D. Sharma, "Operational Calculus on Generalized Two-Dimensional Fractional Fourier Transform," IJEIT, vol. 3, no. 2, pp. 253–256, 2013.

[15] V. D. Sharma and P. B. Deshmukh, "Inversion Theorem of Two Dimensional Fractional Fourier-Mellin Transform," IJACSM, vol. 4, no. 1, pp. 17–24, 2014.

[16] V. D. Sharma and P. B. Deshmukh, "Generalized Two-Dimensional Fractional Mellin Transform," Proceedings/IEEE, pp. 900–903.

[32] A. Gulhane, "Supply chain resilience in the era of digital transformation: A systematic literature review and research agenda," IJERST, vol. 21, no. 4, pp. 1058–1068, 2025, doi: 10.56636/ijerst.2025.v21.i04.3812.

[17] V. D. Sharma and P. B. Deshmukh, "S-Type Spaces for Two Dimensional Fractional Fourier-Mellin Transform," IJASAET, pp. 74–76, June 2015.

[18] A. Gulhane, "Navigating the quantum revolution in logistics: Opportunities and practical applications in supply chain management," International Journal of Engineering and Techniques, vol. 12, no. 3, pp. 553–556, 2026, doi: 10.29126/ijet.2026.v12.i3.553.

[19] A. Gulhane, "Artificial intelligence applications in sustainable logistics and green supply chain management: A bibliometric review," IRJMETS, vol. 6, no. 12, 2024, doi: 10.56726/IRJMETS65006.

[20] A. Gulhane, "Artificial intelligence and blockchain integration for enhancing supply chain transparency, traceability, and resilience," IRJMETS, vol. 6, no. 12, 2024, doi: 10.56726/IRJMETS65016.

[21] A. Gulhane, "Spectral framework based on the FKF transform for supply chain dynamics and resilience," IJCOPE, vol. 2, no. 8, 2026, doi: 10.55041/ijcope.v2i8.140.

[22] A. Gulhane, "A review of resilience in global supply chains," IEJRD, vol. 8, no. 4, 2024.

[23] A. Gulhane, "Shift-invariant spectral analysis of multi-echelon supply-chain lead times via the FKF transform," IJCOPE, vol. 2, no. 8, 2026, doi: 10.55041/ijcope.v2i8.136.

[24] A. Gulhane, "Weaving resilience: Navigating internal and external complexities in modern supply chains," IJIRID, vol. 3, no. 1, pp. 123–128, 2024, doi: 10.5281/zenodo.11491482.

[25] A. Gulhane, "Recent advances in electric vehicle battery technologies: Materials, management systems, and sustainability perspectives," IJSREM, vol. 9, no. 7, 2025, doi: 10.55041/IJSREM51198.

[26] A. Gulhane, "Quantum computing for logistics optimization: Annealing in unit load device configuration and disruption," IJRPR, vol. 7, no. 6, pp. 4643–4648, 2026, doi: 10.55248/gengpi.07.0626.16a57.

[27] A. Gulhane, "Spectral analysis for multi-scale supply chain dynamics and residue-based resonance extraction in hybrid-vehicle systems," IJCOPE, vol. 2, no. 8, 2026, doi: 10.55041/ijcope.v2i8.141.

[28] R. Sharma, R. Katukam, and A. Nagulapally, "Bridging the Linear-Quadratic Gap: A Quantum-Classical Hybrid Approach to Robust Supply Chain Design," arXiv:2601.04095, 2026.

[29] R. G. Ghanem and P. D. Spanos, Stochastic Finite Elements: A Spectral Approach. Springer-Verlag, 1991.

[30] A. Gulhane, "Smart mobility and intelligent transportation systems: Emerging trends, technologies, and challenges," IJSREM, vol. 9, no. 11, 2025, doi: 10.55041/IJSREM53436.

[31] A. Gulhane, "Quantum computing in transportation and logistics: Current state, industrial applications, and future directions," IJSREM, vol. 9, no. 9, 2025, doi: 10.55041/IJSREM52469.

[33] A. Gulhane, "Solar-assisted electric mobility: Design framework and performance assessment of sustainable hybrid vehicle architectures," IJERST, vol. 21, no. 3, pp. 362–368, 2025, doi: 10.56636/ijerst.2025.v21.i03.3594.

[34] A. Gulhane, "FKL transform: Key properties and applications to supply-chain analysis," IJESAT, vol. 25, no. 12, pp. 596–605, 2025, doi: 10.64771/ijesat.2025.v25.i12.3816.

[35] A. Gulhane, "Internet of Things, Artificial Intelligence, and Quantum Computing: A Convergent Framework for Smart Logistics Ecosystems," IJESAT, vol. 24, no. 12, pp. 297–317, 2024, doi: 10.64771/ijesat.2024.v24.i12.3372.

[36] A. Gulhane, "Industry 5.0 and Intelligent Logistics: Transforming Supply Chain Operations through Human-Centric Automation," IJESAT, vol. 24, no. 12, pp. 287–296, 2024, doi: 10.64771/ijesat.2024.v24.i12.3371.

[37] A. Gulhane, "The Future of Vehicles: Solar-Powered Battery Electric Hybrid Vehicle Architecture," Tech Briefs Create the Future Design Contest, entry 10457, 2020.

[38] H. G. Feichtinger, K. Gröchenig, and D. Walnut, "Wilson bases and modulation spaces," Mathematische Nachrichten, vol. 155, pp. 7–17, 1992.

[39] J. Toft, "The Bargmann transform on modulation and Gelfand–Shilov spaces," Journal of Pseudo-Differential Operators and Applications, vol. 3, pp. 145–227, 2012.

